Open Access

Recent Progress in Materials

LIDSEN Publishing Inc.

Research Article

Biocompatibility and Surface Integrity of Zirconia Ceramics Treated by Laser-plasma Driven Shock-waves

Pratik Shukla [1,*], Vincent Zhang [2], Xiaojun Shen [3], Victor M. Villapún [4], Sophie Cox [4], Phil Swanson [2]

1. Ansty Park, The Manufacturing Technology Centre, Ansty Park, Coventry CV7 9JU, United Kingdom; E-Mail: pratik.shukla@the-mtc.org; pratik.shukla@talk21.com
2. Coventry University, School of Mechanical, Aerospace and Automotive Engineering, Coventry CV1 2JH, United Kingdom; E-Mail: Zhang.vincent@outlook.fr; aa1022@coventry.ac.uk
3. School of Electrical and Electronic Engineering, Nanyang Technological University, 50 Nanyang Avenue, 639798, Singapore; E-Mail: xiaojun.shen@ntu.edu.sg
4. School of Chemical Engineering, University of Birmingham, Edgbaston B15 2TT, United Kingdom; E-Mails: V.M.Villapun@bham.ac.uk; s.c.cox@bham.ac.uk

* **Correspondence:** Pratik Shukla; E-Mail: pratik.shukla@talk21.com

Academic Editor: Eugeniusz Sajewicz

Special Issue: Advanced Dental Materials

Recent Progress in Materials
2022, volume 4, issue 4
doi:10.21926/rpm.2204025

Received: April 10, 2022
Accepted: October 17, 2022
Published: November 22, 2022

Abstract

This is a multi-disciplinary paper focused on the preliminary results of deploying laser shock treatment (LST) to ZrO_2 ceramics. This work has significance in several industrial sectors for components that will benefit from strengthening. These components are, namely: dental implants; cutting and drawing tools; valves, bearings, pressure vessels, heat exchangers and high-performance scissors and knives, where modification of hard, brittle materials properties such as that of a ZrO_2, can yield a performance boost. To elucidate the influence of LST on ZrO_2 ceramics, an Nd: YAG laser was used, exhibiting (operating at discrete) laser energies of 17 mJ, 85 mJ and 170 mJ, a 2 mm spot size, a pulse repetition rate of 5 Hz and pulse duration of 10 ns was deployed at 532 nm wavelength. Investigation of ZrO_2 ceramic surface integrity revealed a transition from a crack-free topology to a surface dominated by fractures, as the

laser energy increased from 85 mJ to 170 mJ. Residual stresses obtained by incremental hole drilling (IHD) were measured to be tensile in the upper layer and the sub-surface layer. However, compression of -595 MPa was found in the sub-surface of the ZrO_2 ceramic to a depth of 350 µm after LST, particularly in the transverse direction. Biological analysis metabolic activity measurements, indicated a rise in activity for all samples as the contact time increased (24 h, 3 d and 7 d). The as-received surface revealed a more limited change in metabolism, retaining similar biochemical levels during the first 3 days followed by a slight increase after a week of cultivation, bringing about significant increase in activity in all LST surfaces, relative to the as-received condition. This suggested that a ZrO_2 LST exhibited enhanced cell response, particularly, after 7 days of contact-time. The overall outcome of this introductory paper, not only showed that ZrO_2 ceramics, can be laser shock treated/peened, to induce some possible beneficial mechanical and physical effects, microstructural and surface topography changes, but also showed that LST can facilitate improvement in cell response to the ZrO_2 ceramic. This opens-up, new prospects for treatment of ZrO_2 based ceramics for biological applications such as tooth implant screws, where avoiding fractures from mechanical loading, strength enhancement, as well as biocompatibility are all important.

Keywords
Laser shock treatment; peening; zirconia; ceramics; mechanical behaviour; biological response

1. Introduction

Zirconia (ZrO_2) is a compound of a metal called Zirconium. Pure metallic Zirconium is somewhat soft and flexible (Young's modulus ~95 GPa) in its original form [1]. Zircon is a shiny mineral based on Zirconium. ZrO_2 oxide is the most common compound of Zirconium. The engineering applications of ZrO_2 ceramic are wide and varied [2]. They range from advanced ceramic tube bearing technology, compressors, cutters, pumps, valves and filters, thermal barrier coatings to name a few. ZrO_2 was predominantly used for refractory applications, but it is now widely known for being an excellent material for biological applications, namely: dental implants, dental frameworks, crowns and bridges implant prosthesis [3], as well as hip and shoulder replacements. It has excellent biocompatibility, high strength, with high fracture toughness and slow crack growth characteristics compared to other ceramics. It has high wear resistance, low thermal conductivity and it is also chemically inert. The ability of ZrO_2 to transmit light is also very good [4].

However, problems still exist with these materials, namely: brittle fractures, due to their low resistance to fracture. In clinical applications such as tooth implants, the ZrO_2 ceramic has been known to fail after operating for 2 to 5 years [5], subject to cyclic loading. ZrO_2 ceramics, particularly, deployed in the clinical industry are treated with surface treatments, such as porous coating, large grit alumina particle sandblasting, zirconia sandblasting, alumina sandblasting followed by acid-etching [5]. The sand blasting would enhance the surface properties [6], and these tend to last longer, particularly, sand blasting followed by acid etching (108 months at max) [5]. However, the depth of penetration of sand blasting is not enough and better surface properties are needed that

are induced deeper, thus, long-lasting. This all-in-all, indicates that mechanical properties of zirconia would still requires optimising and clinical application protocol is still not fully known and controllable [3]. In addition, the failure of ZrO_2 implant for instance, require significantly involved surgical procedure to retrieve the failed, but completely osseointegrated implant. This is considerably distressing and painful for the patient as it often includes bone grafting, time for healing, and additional expense. Moreover, reduction in grain size, towards nano dimensions and improved chemical composition can benefit ZrO_2 to become far superior with respect to its properties, that will benefit aforementioned applications in both the engineering and biomedical sectors. Significant number of surface technologies have been deployed to modify the implant morphologies [7]. These are: acid etching, grit-blasting, laser treatment, UV light, CVD, and PVD. Previous work has shown that modification of ZrO_2 ceramic surfaces rendered a significantly rapid osseointegration compared to those that are untreated [7]. With that said, there is limited knowledge as to which surface treatment consequently enhances ZrO_2 ceramic to boost osseointegration, bacterial properties and at the same time, mechanical strength from these specific treatments [7]. Some of the surface treatments adopted are somewhat outdated and involve considerable waste such as grit-blasting [7]. None of these surface treatments have been weighted better over others, in order to enhance osseointegration, but, it has been suggested that roughness, wettability, and surface energy are recommended to enhance the adhesion, proliferation, and differentiation of osteoblasts cells. However, it is suggested that optimisation of surface treatments such as grit blasting, acid etching, and heat treatment should not negatively affect the mechanical properties of ZrO_2 such as fracture toughness and flexural strength and induce micro-cracks. Surface treatment such as grit blasting are preferred to avoid micro-crack formation and additional excessive application of techniques such as acid etching could degrade the ZrO_2 so controlled measures have to be applied [7]. Therefore, the work in this paper explores a laser-based techniques that is cleaner, greener, faster, effective and more advanced. Much work has been conducted, however, using laser surface texturing technology [8], and with the use of continuous wave lasers to modify surface morphologies of ZrO_2 ceramics [9, 10]. However, laser shock treatment applied herein, was inspired by “laser peening”, has not been adopted for this sector. We have therefore explored the laser-ZrO_2 ceramic interaction in this study the direct effects of LST which is a new technique for surface strengthening ceramics. In particular, this method was deployed without pre-or post-heating which tends to increase the complexity and the cost of the process.

Laser shock peening (LSP) is an advanced process, widely used in industry to enhance the mechanical properties of the treated material. Its basic working principle is pre-stressing the material by directing controlled laser pulses at the material surface in order to improve performance, quality and longevity [11, 12]. Pre-stressing materials is well-known for strengthening engineering components, whereby, high-speed particles/balls are imparted at the material to compress the top-layer and introduce residual stresses capable of improving the materials performance. This process is mainly used on ductile metallic materials such as steels, aluminium alloys and titanium alloys for the medical, automotive and aerospace industries [13]. Laser shock peening is an evolution of traditional shot peening in which high-speed balls are replaced by a pulsed laser to generate shock-waves and induce plastic deformation and residual stress within the material [13-15]. Compared to traditional shot peening, LSP ensures induction of higher residual

stresses, greater penetration depths, flexibility and control, resulting in a more effective treatment, albeit, with higher economic costs involved [16].

Laser Shock Peening has been widely used in the industry for the treatment of metallic alloys with many studies elucidating its effect on these (traditional engineering) materials. The ability of LSP to modify the internal stresses of the selected surface is known to enhance many properties such as fatigue resistance [17], fracture toughness [18], hardness or corrosion behaviour [19, 20]. However, the effect of LSP or LST on engineering ceramics is not well understood with only a few published studies available in the literature [11]. The main rationale behind this preference for metallic alloys esteems from the brittleness, low fracture toughness and inability to induce plastic deformation inherent to ceramics, which inhibits their more wide-scale use in many high performance applications that their otherwise desirable mechanical and thermal properties would enable, thus, preventing a more widespread use of ceramics in high-performance applications [9]. Using a controlled laser shock based technique could provide a practical technique to address the inherent (vulnerability) of ceramics to brittle fractures, by enhancing their local surface fracture toughness and reduce their crack sensitivity to expand diverse range of commercial applications.

Recent studies [21-23] have shown that moderate levels of plastic deformation may have been induced in ceramics (under specific conditions) [24-26], leading to better tensile behaviour and enhanced mechanical properties (K_{IC} and hardness) [16, 27]. Other studies [28, 29] confirmed the observation crack length under Vickers micro hardness indentation response, and corresponding reduction after LSP confirming the increase in ductility caused by the introduction of residual stress within the ceramics. Koichi *et al.* [22], performed analysis of LSP strengthening of silicon nitride (Si_3N_4) through a Nd: YAG laser with a 532nm wavelength and has hinted as to plastic deformations induction in the material, resulting in compressive residual stresses. Wang et al. have also reported several studies on laser shock processing polycrystalline alumina ceramics and Silicon Carbide Ceramics [30, 31] and demonstrated dislocation movement, compressive stresses and enhanced fracture strength. Studies conducted by Shukla *et al.* [31], showed improvements in surface roughness, fracture toughness and hardness in laser shock treated Al_2O_3. Further works on silicon carbide conducted by Shukla et al., also confirmed the aforementioned findings and indicated that laser parameters should be properly controlled to prevent an excessive cracking and a beneficial mechanical response. Another study conducted by the same authors [32], has focused on residual stresses in Al_2O_3, revealing an increase in surface roughness and compressive residual stresses, as laser energy was increased. In addition, the density of dislocation increased after LSP, showing plastic or micro plastic deformations [26]. Our more recent studies [32] showed improvements in surface toughness, fracture toughness and hardness in Al_2O_3. Later works on silicon carbide also confirmed these findings and showed that, the right parameters were crucial as with too much laser energy, input the material was damaged. Another study [32] focused on the study of residual stress in Al_2O_3 and showed an increase in surface roughness and compressive residual stress when the laser energy is increased. The dislocation density measured by Cr^{+3} fluorescence increased after LSP, inferring plastic or micro plastic deformation directly under the surface and within the sub-surface of an alumina armour ceramic. Our recent study also explored laser shock treatment of a Si_3N_4 ceramic with a multiple-layer, square-beam [33]. Surface topography, hardness, fracture toughness (K_{Ic}), residual stresses, and microstructural changes were observed. The results showed an increase in K_{IC} of 60%, a maximum of -289 MPa of compressive stress at 50 µm depth and using multiple layers of LST had induced beneficial residual stresses to a maximum measured depth of 512 µm

[33]. Other than that, there has been no published work on the influence of LSP on ceramics, particularly, on ZrO_2 ceramics. This study intends to understand how ZrO_2 behaves under LST and more specifically, regarding hardness, fracture toughness and the change in residual stresses. This work reveals the viability of LST/LSP to overcome the natural limitations of ceramic materials, expanding their use more widely in the industry. It also encourages other researchers to dwell deeper into the topic, as well as expanding the usage and applicability of these materials in the wider industrial sectors with this new capability suitable for brittle materials.

The rationale for the undertaking the biological work is due to the fact that ZrO_2 ceramic is a heavily deployed materials for dental [34, 35], as well as other medical applications [36]. Fundamentally, both the mechanical properties and biocompatibility hold significance spanning biomaterial to medical or dental applications [34]. The state of the surface post any processing technique dictates the biocompatibility of the ZrO_2. In addition, the mechanical strength is dictated by elastic, plastic, thermal, chemical, and kinetic properties as well as tensile residual stresses induced from its processing technique. Thus, surface treatments such as sand blasting, machine grit-blasting, machining, plasma spraying, acid etching, and anodising are desirable to not only enhance the strength, but also influence its biocompatibility [26, 34, 37, 38]. One of the biggest issues with these applications is that surface treatment such as shot peening for example or alternative technology for enhancement are not so superior compared to a laser shock based process, namely: laser shock peening and so it could; a) render benefits not only from a view point of surface and sub-surface enhancement and; b) the effect of topographical changes that may enhance the biological response of the ZrO_2; c) it is selective, advanced and can be faster, greener, and cost-effective in the long run as (high capital cost) laser technology will in turn pay for itself and render a competitive advantage. Laser shock treatment will also enable better performance from the ZrO_2 part being treated, but will also enhance the longevity and end-user satisfaction, facilitate pain and cost saving by needing less replacement (second surgery).

2. Methodology

2.1 Background of the Zirconia Advanced Ceramic

The material used was commercial grade zirconia (ZrO_2) ceramic, having been cold isostatically pressed to a dimension of 50 × 10 × 5 mm (length × width × thickness), provided by Shanghai United Technology. The mechanical properties and characteristics are shown in Table 1. The calculated Hugoniot Elastic Limit (HEL) was 4.55 GPa using established methodologies from previous work [34], with a yield strength and Poisson's ratio of 2.87 GPa and Poisson's ratio of 0.27 for Zirconia. This meant that for plastic deformation to occur in the surface, sub-surface of the material, the laser shock pulse pressure has to exceed this threshold value range (4.55 GPa or 2.87 GPa), if it is assumed that the yield model developed (for the onset of metal plasticity is still valid for ceramics, an area of some conjecture). Table 1 shows the properties of the ZrO_2 ceramic.

Table 1 The mechanical properties of ZrO_2 ceramics used in this work.

Item	Unit	ZrO_2
Density	g/cm^3	6.05
Thermal expansion coefficient	$10^{-6}/k$	10.5

Modulus of elasticity	GPa	210
Poisson's ratio		0.30
Hardness	(HV)	1200
	(HRC)	70
Flexural strength (700°C)	MPa	300
Compressive strength (700°C)	MPa	2100
Fracture toughness	MPa. $m^{1/2}$	10.0
Thermal conductivity (500°C)	W/mk	2
Specific resistance (600°C)	$\Omega mm^2/m$	10^{15}
Maximum operation temperature	°C	550
Anti-chemical corrosion		Strong
Stress cycle (50% damage probability)	Times	10^5
Size stability (temperature)		--
Operating centrifugal force		Highest
Unlubricated friction		Low
Magnetism		No
Rolling contact fatigue failure mode		Fragments

2.2 Microstructural Analysis

Both the high and low magnification images were taken of the ZrO_2 ceramic, before and after laser shock treatment. The low magnification images were taken using a Lyca (Milton Keynes, UK) microscope at ×10 and ×20 magnification. These images are important to observe any major micro cracks and the surface morphology. Thereafter an SEM was used to observe the microstructure at high resolution. The Scanning Electron Microscope (SEM) used was a Hitachi, TM4000 table top microscope). Samples were first sputter coated with gold so they become electrically conductive for SEM analysis.

2.3 Topographic Analysis

The surface topography of the ZrO_2 before and after laser shock treatment was investigated to understand the effect of plasma-driven shock waves. This in turn, is a by-product and a consequence of the laser shock processing techniques. A focus variation technique with Infinite Focus Veriation (IFM 2.15; Alicona) was used to analyse the topography. This evaluated a three-dimensional (3-D) surface, producing 3-D surface profiles and roughness characteristics of the laser shock treated ZrO_2. The process utilised a laser beam of 2 mm diameter. This travelled to length of 8 mm across the width of the substrate. The scanning speed used was 33.33 $\mu m.s^{-1}$.

2.4 Laser Shock Treatment Set-up

The laser shock treatment was conducted with a 2.7 J, Q-Switch, Nd: YAG laser (LPY7864-30, Litron Laser Ltd., Rugby, England). The wavelength used for was 532 nm at a pulse repetition rate of 5 Hz and a laser pulse duration of 10 ns. The laser energies used were 17 mJ, 85 mJ and 170 mJ. The spot size was constant at a diameter of 2 mm and these conditions yielded a laser intensity varying from 0.057 GW/cm^{-2} to 0.54 GW/cm^{-2}, respectively, for all the conditions and a shock pulse

pressure detailed in Table 2, alongside more detailed laser properties. Figure 1 (a) showed an optical image of the experimental set-up, (b) is the schematic of the process effects.

Table 2 Experimental parameters used in the current study for the laser shock treatment of ZrO_2.

Parameters	Values
Pulse energy (J)	17 mJ, 85 mJ, 170 mJ
Laser power intensity (GW.cm^{-2})	0.054 GW/cm^{-2} @ 17 mJ (Crack-free surface) 0.270 GW/cm^{-2} @ 85 mJ (micro-cracking) 0.54 GW/cm^{-2} @ 170 mJ (Cracking)
Radiance Density (W/mm^2/Srt/µm)	0.48 @ 17 mJ 2.40 @ 85 mJ 4.81 @ 170 mJ
Shock Pulse Pressure (GPa)	0.40 GPa @ 17 mJ 0.90 GPa @ 85 mJ 1.27 GPa @ 170 mJ
Spot diameter (mm)	2 mm
Pulse repetition rate (Hz)	5 Hz
Pulse duration (ns)	10 ns
Wavelength (nm)	532 nm
Pulse over-lap	40%
Ratio of thermal to internal energy [30]	0.1

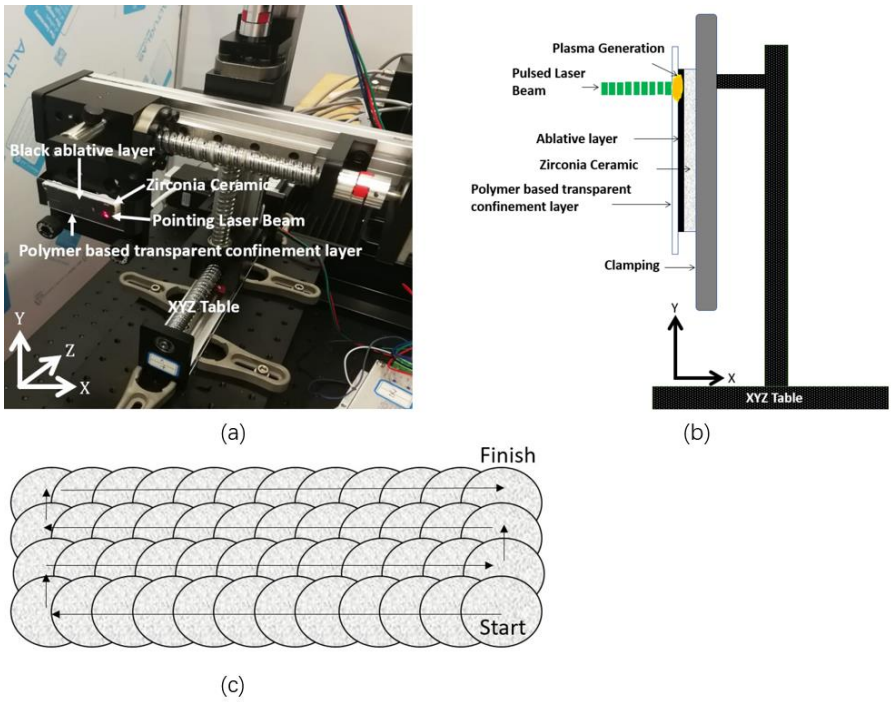

Figure 1 Details of the laser shock treatment including (a) an image and a (b), the schematic of the experimental set-up and (c) the laser shock treatment strategy deployed.

The laser treated area was 9 mm × 40 mm in a rectangular pattern as shown in Figure 1 (c). The shock pulse pressures were calculated using Equation mentioned elsewhere [33]. The LST work was conducted on a 45 × 10 mm patch for the 3 different energies following a zig-zag pattern. The absorbent coating used as the transparent confinement overlay was a layer of permanent black-ink coating. This black-ink was measured to be about 5 µm thick and was removed with the LST. The transparent polymer was used as a tampering with a thickness of about 1.5 mm.

2.5 Hardness Testing and Fracture Toughness Measurements (K_{IC})

Hardness was measured using a classic Vickers hardness tester with a load of 98.1 N. The hardness test was performed 10 times with an average and standard deviation reported. Fracture toughness (K_{1c}) was determined using indentation technique mentioned elsewhere [39]. From all available methods [32], Antis *et.al*'s [40] technique was selected to carry out the present work, following the detailed review of work by Shukla *et al.* [10, 41]. The Equation specifically used was for the deermination of K_{Ic} was of Anstis, Chantikul, Lawn & Marshall's Equation (K_{1c} = 0.016 $(E/Hv)^{1/2}$ $(P/c^{3/2})$) [40], where, E is the Young's Modulus, HV is the hardness, P is the load (N), c is the crack lenth.

2.6 Residual Stress Measurements

2.6.1 Incremental Hole Drilling

A custom made incremental hole drilling (IHD) machine (Stresscraft, UK) was used for residual stress measurement of both the laser shock treated and the as-received ZrO_2 surface. Each sample was prepared for the incremental hole drilling experiments using the standard procedures. The strain gauge used was a type EA-XX-031RE-120 from Vishay Ltd. (Sunderland, UK) as shown in Figure 2. Due to small pattern size, measurement error can be magnified by slight miss-location of drill hole, however, this was a specialised application and the sample size demanded that only this strain gauge was to be deployed as other gauges were not suitable being too large. The position of the strain gauge was located as shown in Figure 2 for both the untreated and the laser shock treated ZrO_2. A diamond drill of 1.66 mm in diameter was used to produce the incremental hole drilling. The depth of drilling was 1.86 mm and the data obtained for 1.24 mm depth of residual stress values. Strain was measured in X-and Y-axis and then tabulated into stress values using the stress craft software package.

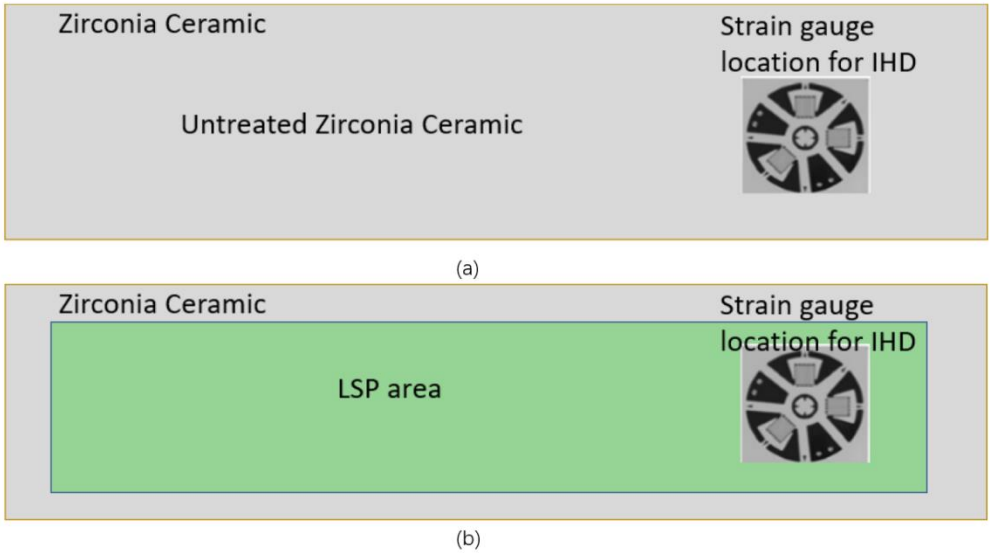

Figure 2 A schematic images of the location of the strain gauge adhered to both the untreated and laser shock treated ZrO_2 surfaces.

2.6.2 Residual Stress Measurement by Indentation

Residual stresses at the surface were calculated using an indentation crack-based approach as proposed by Marshall *et al.* [42]:

$$\sigma_r = \frac{\sqrt{\pi}\chi}{2m\sqrt{c}}\left[\frac{K_{1c}}{\chi} - \frac{P}{c^{\frac{3}{2}}}\right] \quad (1)$$

With χ a material and indenter dependent constant given in [43]:

$$\chi = 0.016\left(\frac{E}{H}\right)^{0.5} \quad (2)$$

where the correction m is set to 1 which means a neglect of free surface-effects and a homogeneous residual stress field [44]. H is the hardness in GPa and E is the elastic modulus (GPa); P = indentation load (N), c = crack length (µm). E is the Young's modulus in GPa and H is the hardness in HV.

2.6.3 Biological Testing

Influence of laser shock treatment on the cytotoxicity of ZrO_2 ceramic was studied using a human osteosarcoma cell line (Saos-2, P13). SAOS-2 was selected based on the common use of ZrO_2 in dental implants, dental frameworks, crowns or implant prosthesis. While other tissues will be in contact with these devices, their main objective is to procure a strong and stable union between bone and implant. For this reason and as a first step in understanding the effect of peening in this material, the established human osteosarcoma cell line SAOS-2 was selected. Before the inoculation samples were degreased with pure ethanol in an ultrasound bath for 10 min, disinfected by autoclaving, immersed in pure ethanol for 5 min and dried under UV light. Samples were inoculated with 20000 osteoblastic cells and incubated for 40 min (37°C and 5% CO_2), to allow initial cell adhesion to the substrate. Subsequently, samples were covered with Dulbecco's Modified Eagle

Medium (10% Fetal bovine serum, 12% L-Glutamine and 1% penicillin/streptomycin) and cells cultured for up to 7 days at 37°C and 5% CO_2. Media exchange was carried out every two to three days. To analyse the viability and proliferation of cells deposited on the samples, Alamar Blue (Fisher Scientific UK Limited) and fluorescence imaging were performed. A 10% of the medium amount of Alamar Blue was inoculated and left in an incubator for 4 hours at 37°C. 100 µL was taken onto a 96 well and fluorescence read at 570 nm excitation and 590 nm reading wavelengths. Measurements were developed in triplicate with mean and standard deviation reported. For fluorescence imaging, each sample was washed gently three times with 10 mM PBS, stained with 200 µL of 5 mM calcein-AM (VWR International, USA) and 1.5 mM propidium iodide (Thermo Fisher scientific, USA) solution and incubated for 30 minutes. Imaging was carried out using an EVOS M5000 Imaging System (Thermo Fisher Scientific, UK) with ×5 and ×20 magnification. ANOVA analysis was performed on the metabolic activity measurements after 7 days of seeding with the figure and text changed accordingly. The statistical analysis for the biological assays was conducted with SPSS (IBM Corp. Released 2015. IBM SPSS Statistics for Windows, Version 23.0). Similarity of variances was checked with Levene's test and, if not violated, ANOVA-I was performed followed by Turkey's post-hoc with alpha level 0.05. In case that similarity of variances cannot be assumed, mean comparison was analyzed through Welch's test and Games-Howell's post-hoc.

3. Results and Discussions

3.1 Macroscopic Evaluation of the Surface after Laser Shock Treatment

Observations were conducted over a range of magnifications using optical microscopy, to understand the microscopic effect over the surfaces of the ZrO_2 ceramic at low resolutions, to evaluate if the laser shock treated brittle ceramic is free from laser-shock induced defects. An initial visual inspection of the samples after LST was first carried out to determine the presence and length of cracks induced in the ZrO_2 substrates. Figure 3 illustrates an optical image of a plan view of the samples whilst, Figure 4 shows clearly the effects of laser energy upon the surface of the ZrO_2 ceramic from the optical images. The effects become more apparent as the selected laser energy rises to 85 mJ, beyond which visual macroscopic signs of burning were readily observable.

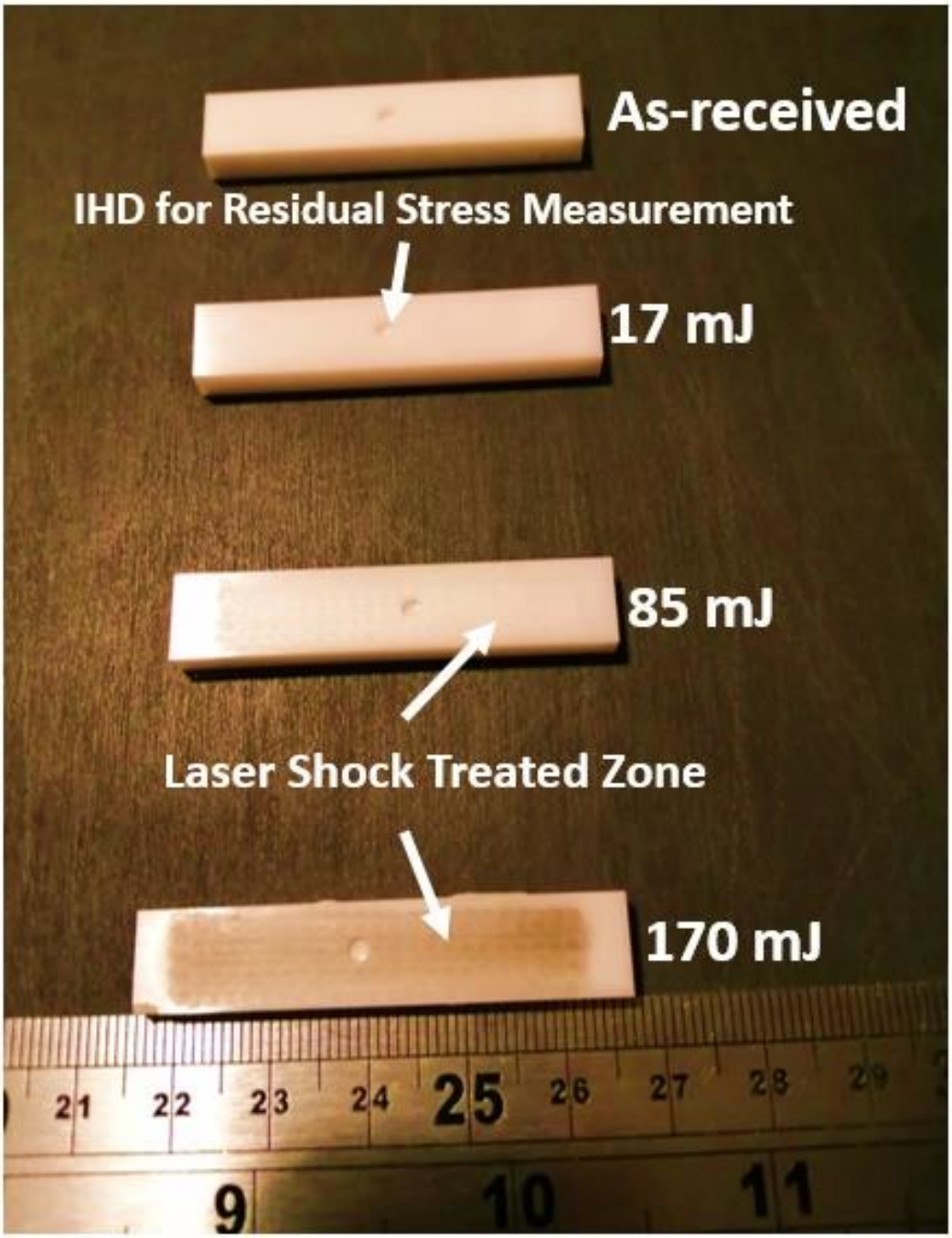

Figure 3 Optical image of the ZrO_2 Ceramic samples treated by different laser energies.

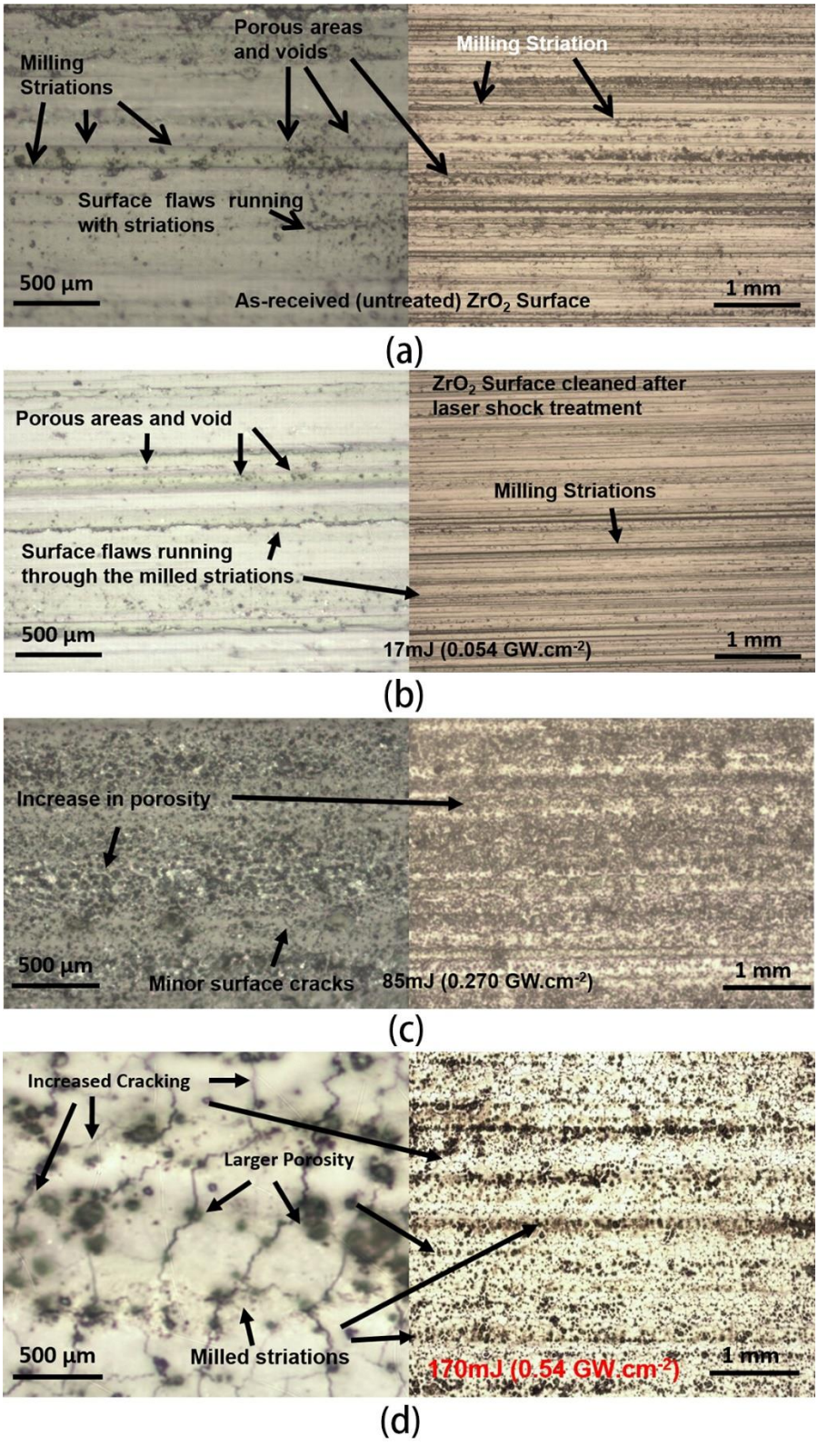

Figure 4 Optical images of the ZrO_2 surfaces in the as received (a), and laser shock treated surfaces at 17 mJ (b), 85 mJ (c), and 170 mJ (d).

These marks (as-received striations) are still apparent in the different samples after LST due to higher LST energy, but they become less prominent as the laser power increases, particularly in the 85 mJ (Figure 4 (c)) and 170 mJ (Figure 4 (d)), peened samples. The surface of the lower energy

treated sample (Figure 4(a)) consists of cracks but, further rise in power to 85 mJ revealed the presence of small cracks at different locations. These cracks become more apparent on the 170 mJ sample where big cracks homogeneously distributed on the peened surface can be observed (Figure 4 (d)). Laser shock peening is known to cause the disappearance or attenuation of the as-received machining marks which could reduce the surface properties of the material. The surface integrity obtained from the as-received and laser treated samples indicated that the striations were reduced through laser shock peening. This effect was especially relevant for the 85 mJ and 170 mJ samples, although, such high laser energies were unable to be completely absorbed by the base material, as indicated by the higher presence of cracks as the laser power was increased. To enhance the surface finish of the base material while preventing crack generation; it was found that laser energies between 17 mJ to 85 mJ are sufficient. For future studies it is recommended that the very top of the laser shock treated ZrO_2 ceramic, should be removed post LST with sand blasting/micro-shot peening (or chemical/acid etching) to remove the initial cracked layer from the as machined surface condition. Once this operation performed, the top surface will have lesser defects and susceptibility for fracture when exposed to laser shock driven pressure pulse.

Based on observations from optical microscopy presented in Figure 4, machining sourced striations were diminished *via* LSP treatment, particularly, at higher laser peening energies (85 mJ and 170 mJ). It is suggested that surface cracking produced at the highest laser energy tested is due to the higher magnitude of mechanical shock induced into the substrate surface at higher laser energies/intensities beyond applying 17 mJ. To obtain a crack-free laser peened surface, further studies with energies between 17 and 85 mJ need to be conducted. Figure 5 shows SEM images of the untreated (a) and crack-free laser shock treatment in (b) at 17 mJ of laser energy. What this indicates is that, the surface integrity is slightly enhanced and there is an effect of striation removal and flattening as well as the surface integrity being enhanced possibly through some surface cleaning, other surfaces treated with 85 mJ and 170 mJ rendered increase in porosity and surface micro cracking respectively.

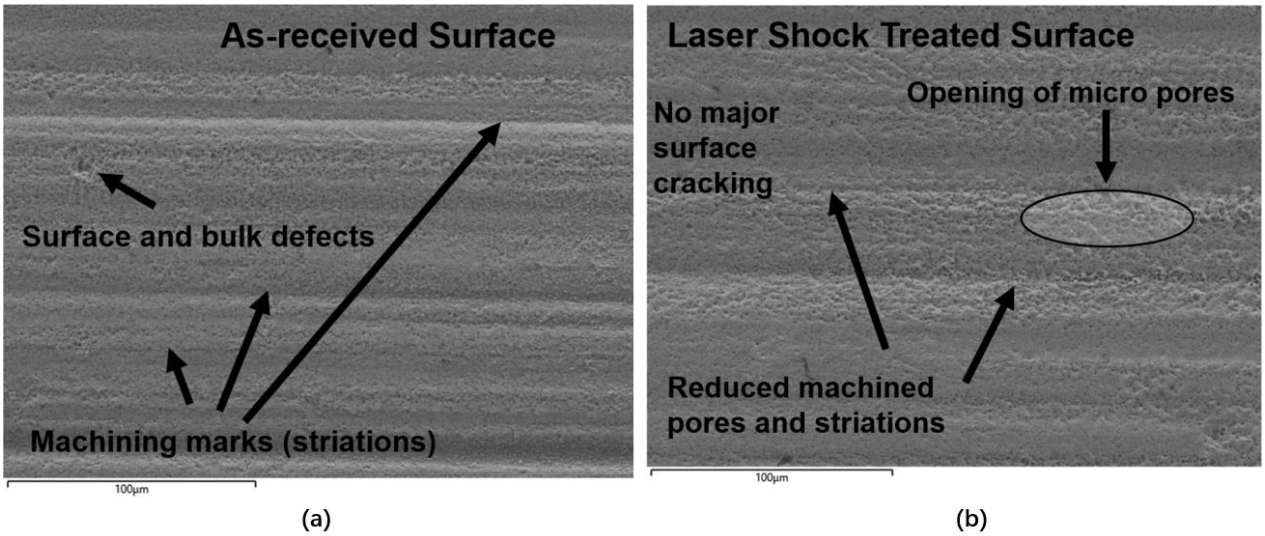

Figure 5 Scanning electron micrograph of the as-received surface of the ZrO_2 in (a) and (b) the laser shock treated surface.

3.2 Surface Roughness and 3-D Profiles

Following the SEM images are the 3D scan mapping images of samples using the Alicona infinite focus variation system (see Figure 6). These compare the optical images with what is seen on 3D profile maps, as well as line profiles traversing across the samples.

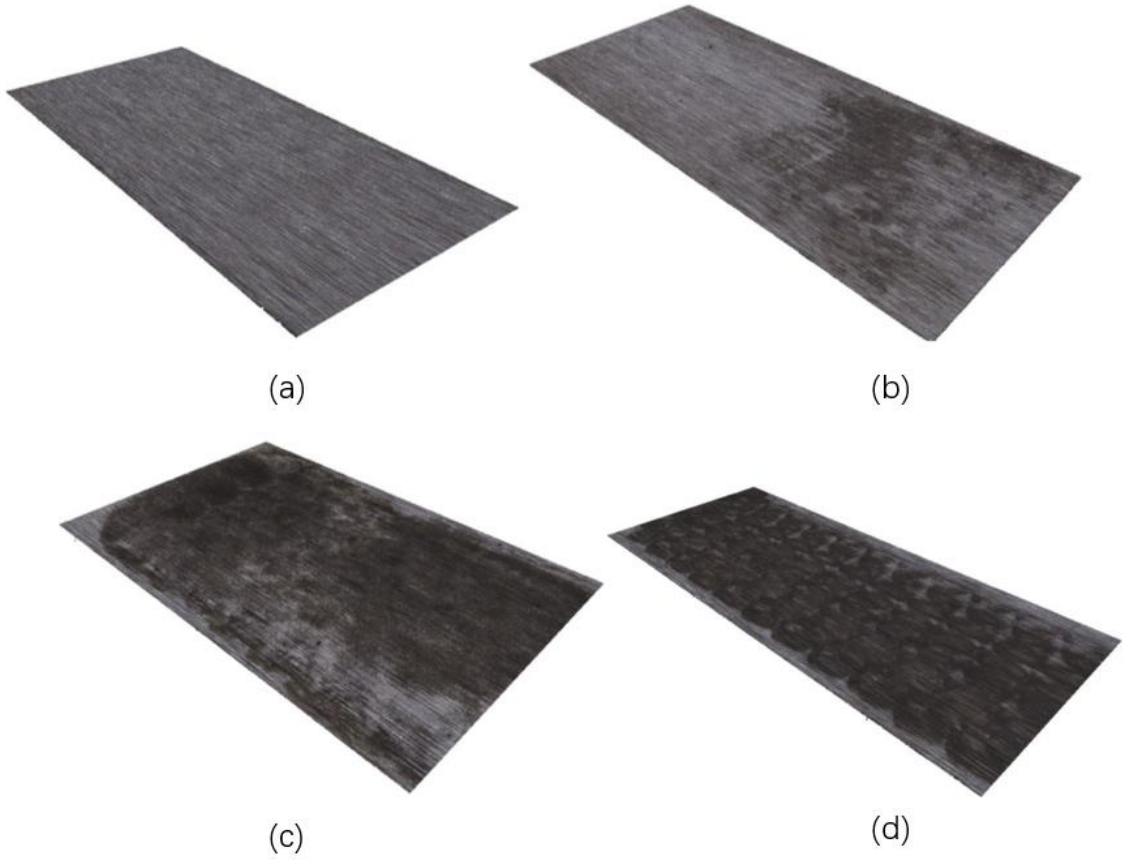

Figure 6 Topographical Analysis showing the roughness characteristics before and after LST; (a) as-received; 17 mJ (1%) in (b); 85 mJ (5%) in (c); and 170 mJ (10%) in (d) of ZrO_2 ceramic.

Figure 7 presents a graph of surface roughness (Ra), with respect to the applied conditions of as-received surface and the laser shock treatment at 17 mJ, 85 mJ and 170 mJ respectively. It is evident that the roughness reduces with increasing laser energy, where the as-received surface (Ra) was measured to be 1.84 µm, 1.20 µm at 17 mJ and 0.77 µm at 85 mJ and 0.84 µm at 170 mJ respectively. There is a slight dip in the roughness between 85 mJ of energy applied compared to 17 mJ. This can be attributed to the removal of distinct striations and the surface flaws that were present on the as-received surface. As the energy increased the removal and flattening of the machining marks and striations rendered a decrease in the Ra value, and resulted in laser shock treated surface becoming significantly smoother. This appears to be a general trend in the results observed in Figure 7 compared to the as-received surface which was measured to be the roughest. After 85 mJ, the results of 170 mJ treated surface was slightly increased. Given to the increase in surface cracking at 170 mJ, the roughness rose higher than the 85 mJ surface, however, it was still considerably lower

than that the as-received surface. This indicated the laser shock treatment was producing a smoother surface.

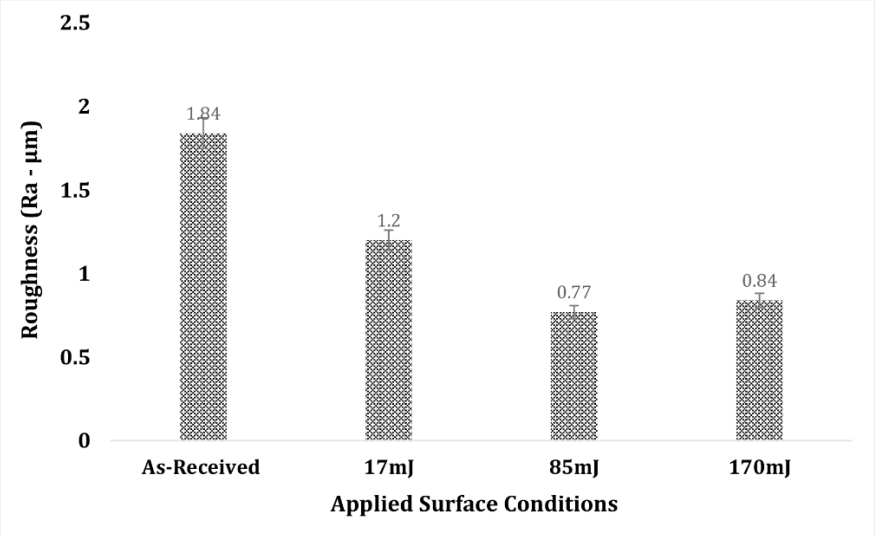

Figure 7 Surface roughness characteristics of the laser treated and the untreated surfaces of the ZrO_2 ceramic.

3.3 Hardness and Fracture Toughness

To further expand the surface analysis previously presented, the influence of laser peening on the hardness of ZrO_2 was studied graphically (Figure 8). The hardness measurements showed a decrease after laser shock peening which corresponds with previous findings. This is attributed to the surface fractures that were found onto the ZrO_2, particularly, when exposed 170 mJ energy and to somewhat 85 mJ laser energy. The hardness of the as-received zirconia is 14.07 GPa, immediately decreasing to 13.37 GPa for 17 mJ, 13.51 GPa for 85 mJ and dropping to a minimum of 12.94 GPa for 170 mJ. This represents a decrease of respectively 5%, 4% and 8% respectively compared to the baseline hardness obtained in the as-received sample, suggesting to the introduction of tensile residual stresses in the upper layer of the sample. A drop in fracture toughness would be more indicative of tensile residual stresses- drop in hardness could be related to re-configuration of the surface dislocations sub-structure from the plasma-induced shock wave. The as received sample (machined surface) may have a dislocations sub-structure that is re-configured (reduced akin to a traditional recovery process) by the LSP induced shock wave. The presence of tensile stress is indeed a factor [30] favouring the penetration of the indenter deeper into the material, thus leaving a larger and deeper depression and correspondingly longer hardness test (Hv) generated crack lengths. The reduction of the surface hardness due to the laser shock peening is an unexpected phenomenon that occurred even at low laser energy (17 mJ) without any visible influence of LSP. Previous work has shown that LSP tends to improve surface hardness [32]. ZrO_2 is a polymorphic ceramic and can adopt different crystal structures as a function of temperature. However, laser generated shock waves may be able to modify the crystal structure, so a meta-stable structure can be generated at room temperature due to the mechanical provocation of the laser sourced shock wave.

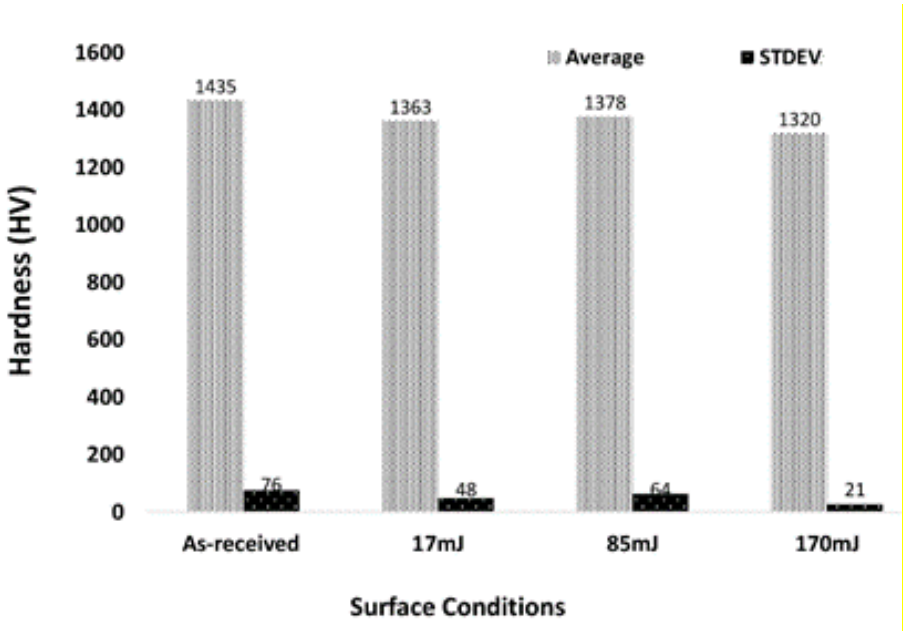

Figure 8 A graphical representation of mean hardness and standard deviation obtained from ZrO_2 ceramic substrates in the as-received-untreated condition and laser shock treated at the three laser energies indicated.

The calculated surface fracture toughness of the different samples is depicted in Figure 9. Fracture toughness values obtained via the hardness testing technique are influenced by harness testing generated crack lengths shown in the previous section. The as-received sample's fracture toughness is calculated as 4.20 MPa.m$^{1/2}$. When the laser energy is 17 mJ (and when the crack length - induced from the hardness testing indentation has decreased) the calculated fracture toughness increases to 4.37 MPa.m$^{1/2}$. This represents an increase of 4% of the fracture toughness compared to the as-received sample. When the laser energy is 85 mJ, the fracture toughness calculated is 4.28 MPa.m$^{1/2}$ as expected, it is lower than in the 17 mJ sample, but higher than the as-received one as the average crack length is in between that from the 17 mJ and as-received sample (see Figure 10). This represents an increase of 1.9% in fracture toughness compared to the as-received sample. For the 170 mJ laser shock treated sample the fracture toughness drops heavily down markedly to 3.58 MPa.m$^{1/2}$ which is a decrease of 14.7% in regard to the as-received sample. This occurred naturally due to the onset of larger surface cracks from the laser shock treated region of the 170 mJ laser energy shock treatment.

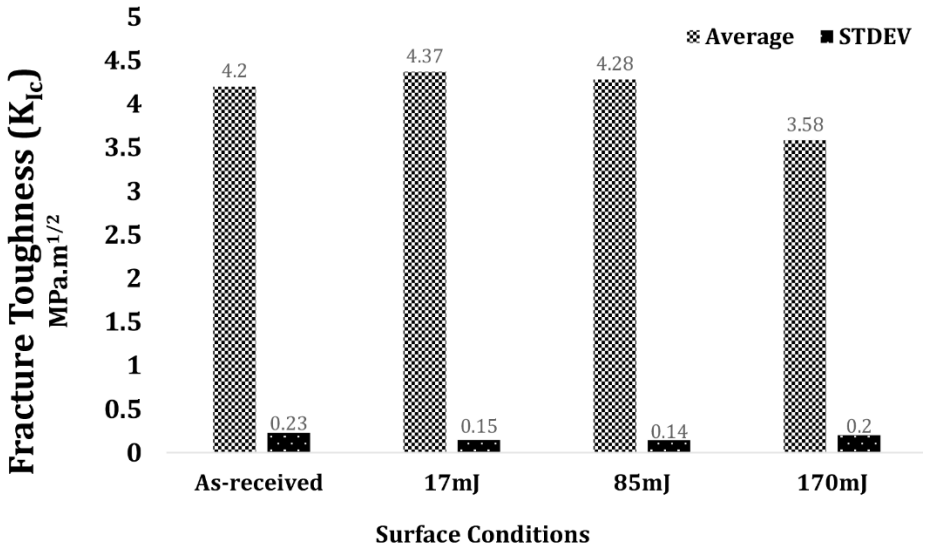

Figure 9 Surface fracture toughness of the as-received, untreated and laser shock treated ZrO_2 ceramics for various laser energies, calculated from the Anstis, Chantikul, Lawn & Marshall Equation shown in section 2.5.

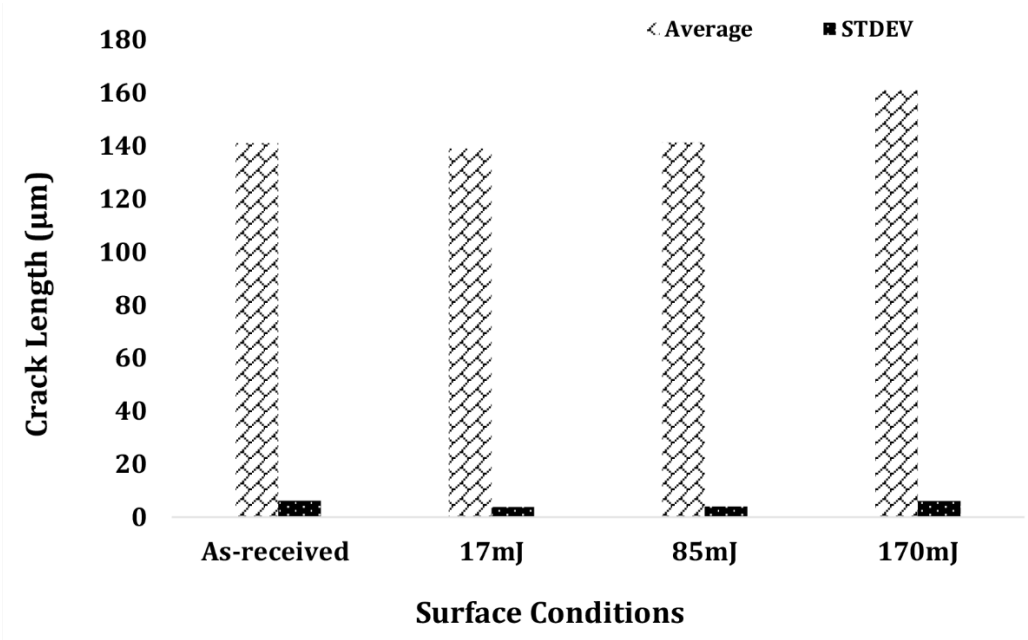

Figure 10 Shows the crack lengths of laser shock strengthened ZrO_2 with 17 mJ, 85 mJ, and 170 mJ and the as-received surface.

3.4 Residual Stress Measurements

3.4.1 Residual Stress Profile by Incremental Hole Drilling Method

Calculated values of both axial (σ_1) and transverse (σ_3) direct stress were represented in Figure 9 (this gives fracture toughness values **not** values of σ_1 and σ_3) for the as-received (untreated) and all the laser shock treated ZrO_2 ceramics. A profile for the residual stress was obtained for each sample using the incremental hole drilling method depicted in Figure 11. The main goal (as widely known)

of LSP is to introduce compressive residual stresses on the surface and sub-surface, in order to, enhance mechanical response and improve surface integrity and resistance to crack initiation from the surface. As shown in Figure 11, on the surface/sub-surface residual stress for the as-received surface was revealed to be a pseudo-sinusoidal, single cycle around a mean value = 0 MPa (with an approximate amplitude of + 50 MPa through the bulk, to a depth of ~1000 µm).

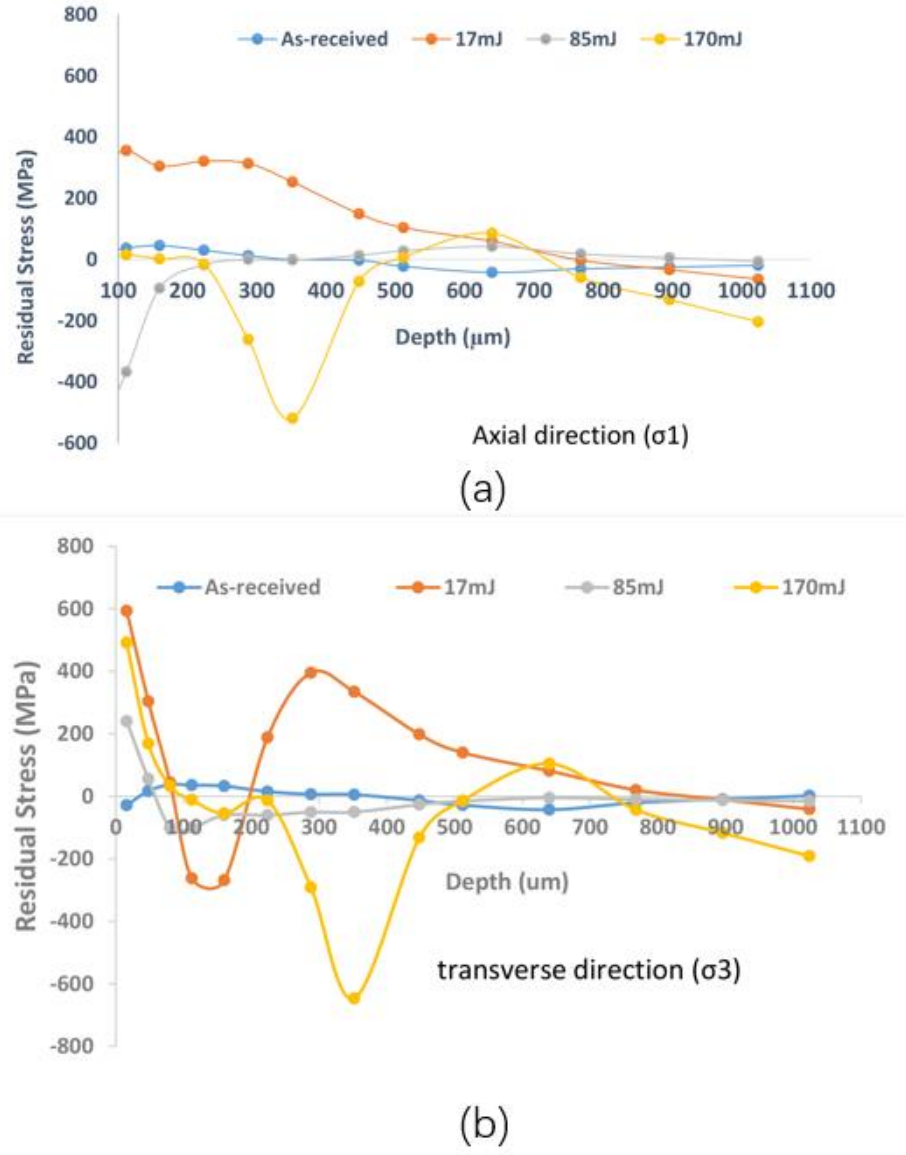

Figure 11 Residual stress on the Laser Shock peened ZrO_2 ceramic with as-received, 17 mJ, 85 mJ, and 170 mJ laser energy measured using incremental hole drilling, σ_1 = axial direction in (a) and σ_3 = transverse direction in (b).

Tensile residual stresses are introduced in the surface layer of all three samples (i.e. those treated at 17 mJ, 85 mJ and 170 mJ) after LSP. This is most likely the reason why the hardness test indent size has increased in all three samples after laser shock treatment as a surface tensile stress is a factor contributing to the increased penetration of the indenter in the material [45]. It is therefore, the main factor accounting for the decrease in surface hardness observed in Figure 8. The presence of tensile stresses, especially within the 17 mJ treated sample; where the surface was not damaged

could possibly be attributed to the fact that the lower intensity shock-waves induced by the plasma, produced by the laser shock treatment bounces back to the surface, hence, introduced tensile stresses along the way [41]. However, the likelihood of this is scares and a more likely cause for the presence of tensile residual stress near the surface is that the surface is damaged due to high brittleness and crack sensitivity after being exposed to the laser shock.

As shown in Figure 11 (a) and Figure 11 (b), compressive residual stresses have been introduced to greater depths within the samples to 85 mJ and 170 mJ of laser energies. For the 17 mJ laser energy treated sample, compressive residual stresses, are mostly found on the transverse direction reaching residual stress (σ_3) values around -270 MPa at a depth of 135 µm as shown in Figure 11 (b). This was not the same for the axial direction (σ_1) for the 17 mJ sample as compressive stress was found at the surface up to +375 MPa which then relaxed and reduced in magnitude through the sub-surface (0 MPa at 900 µm depth).

On the 85 mJ treated sample, the compressive residual stress was mainly found to follow the axial direction (σ_1) with values nearly -400 MPa in the vicinity of the surface (see Figure 11 (a)), whilst in the σ_3 graph (for 85 mJ) showed the tensile stress of 275 MPa on the surface which eventually showed compression of -100 MPa at 75 µm depth.

As for the 170 mJ sample, the compressive residual stress were over -600 MPa at a depth of 350 µm as illustrated in Figure 11 (b) in the transverse direction (σ_3). Comparatively, for the σ_1 direction, the residual stress for 170 mJ was 575 MPa, at a depth of 350 µm. It is obvious that the residual stress measured in with 170 mJ treated samples was somewhat similar in both axial and transverse direction which was not the case for the curves for 17 mJ and 85 mJ. With that said the curve for as-received samples was also similar in both the measured directions.

The results displayed by those measurements in the transverse direction are more promising: compressive residual stresses are being introduced inside the material with LST and the amount increases with the applied laser energy and the stress seems to be introduced deeper as the energy of the laser increases. So, except for the upper layers, the results showed material sub-surface compressive strengthening particularly with 170 mJ in both the measured directions. These results in turn have not been found before, thus, open an avenue for further research. Repetition of the results herein, will verify the findings. Regards to the upper layer in residual tension; this can be removed with another surface treatment for example blast cleaning – which would bring to the compressed region that will be more resistant again the onset of a potential load. This can be done with the use a micro shot peening treatment as demonstrated by Shukla *et al.* [6], were the micro shot peening of ZrO_2 ceramic resulted in the removal of the upper layers of the material. Upon using this kind of process would be beneficial as the material retains the improvements induced by the laser shock treatment, while the problematic areas would be removed by micro shot peening. Although, it can be noted that removing the surface tensile region may cause a re-distribution of the residual stress profile.

The fact that compressive residual stresses are present hints to a degree of plastic or micro-plastic deformation inside the material, even when the shock pulse pressure generated by the different parameters was not high enough to overcome the HEL of the ZrO_2 ceramic. The theory behind the HEL and how plastic deformation is induced by LSP is well known, and well suited for the laser shock peening of metals [12]. However, there are a lack of studies dealing with such theory in ceramics, thus, the process of plastic deformation in these materials is relatively unknown and currently not well understood. Therefore, the theory used is the same as the one suggested for

metals (which obviously is a potential source of discrepancy when applied to ceramics), but better understanding and further studies are needed in order to conclude if the use of HEL and metal plasticity theory is applicable for brittle ceramic materials.

3.4.2 Residual Stress by Indentation Method

The residual stress method based on indentation is an estimate of stress fields at the depth of the indent (see measured values in Figure 12, for laser shock treated ZrO_2 in this work). Considering the differences between the different depth, we can assume that all the residual stresses measured where conducted at a depth of 16.5 µm in order to compare them to each other.

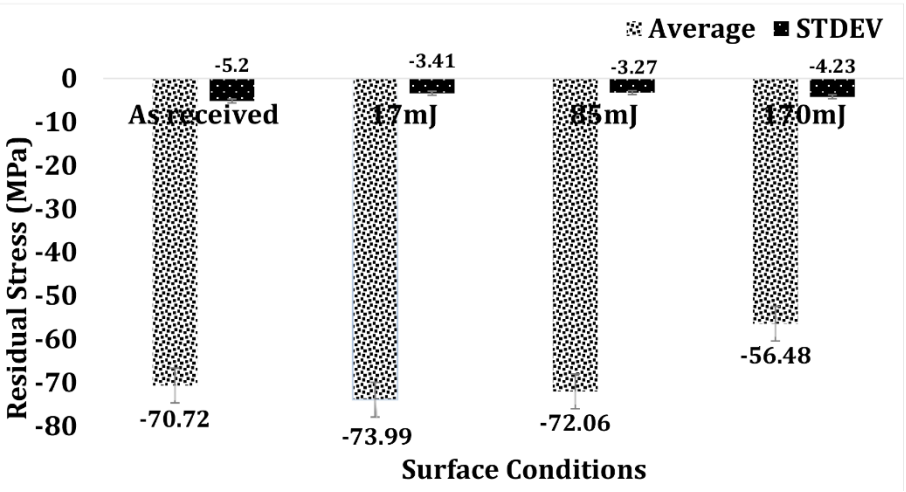

Figure 12 Residual stresses estimated through the indentation method for the as-received, untreated and laser shock peened ZrO_2 ceramics surfaces for various laser energies.

Comparison between hole drilling and indentation methods reveals vastly different results. Residual stresses obtained through indentation at a depth of around 16.5 µm are -70. 72 MPa for the as-received ZrO_2 sample, indicated that compressive residual stresses are already present inside the sample. The amount of compressive residual stresses increases to -73.99 MPa for the 17 mJ laser shock treated sample, which represents a 4.6% increase over the as-received condition. However, a rise in laser energy to 85 mJ leads to a slight change in residual stresses to -72.06 MPa or a 1.9%, increase in compressive residual stress over the as-received sample. Further increase in laser energy, 170 mJ, results in a large drop in compressive residual stress to -56.48 MPa or a 20% decrease compared to the as-received sample.

An increase of compressive residual stress can be observed in the 17 mJ and 85 mJ sample, but the increase is quite small compared to the change observed with the hole drilling method. This is somewhat explained by the equation used for this calculation ($K_{1c} = 0.016\ (E/Hv)^{1/2}\ (P/c^{3/2})$), as it is heavily tied in with crack length and fracture toughness and therefore, may follow the same trend as those two parameters. If these values are correct, the increase in compressive residual stress near the surface in the 17 mJ and 85 mJ samples could explain why the crack length and the fracture toughness improved in those samples. Compressive residual stress will indeed restrain crack growth and, thus, improving the fracture toughness. However, this would also improve hardness, which was not noticed.

An explanation on the disparity of results between the two methods is because done at vastly different scales. The hole drilling method measures the residual stress around a hole with a 2 mm diameter, whereas, the indentation method measures the residual stress around an indent of around a hundred micrometre span. This disparity in scale means that the two measures are quite unrelated and that they cannot be truly compared. Further studies at both macro and microscopic level should be done in order to obtain a better understanding of the residual stress behaviour inside ZrO_2 after LST.

3.4.3 Biological Test Evaluation

To analyse the potential application of laser peened ZrO_2 as a biomedical material, cell viability of SAOS-2 cells was studied (Figure 13). Metabolic activity measurements through the use of the reagent AlamarBlue (Figure 13 (a)) indicated a rise in activity for all samples as the contact time increases (i.e. 24 h, 3 d and 7 d), however, these changes are dependent on the base material and treatment. Control polymeric slides where used to provide a comparison baseline with a non-toxic material, revealing a rapid rise in activity after 3 days followed by stagnation. The as-received surface reveals a more limited change in metabolism, retaining similar biochemical levels during the first 3 days followed by a slight increase after a week of cultivation. In contrast, more prominent changes could be detected on the laser shock treated substrates with all samples revealing a steep rise in metabolic activity as the incubation time increased. More interesting is to notice the significant increase in activity in all laser peened samples relative to the as-received condition, suggesting that this surface treatment enhanced cell response.

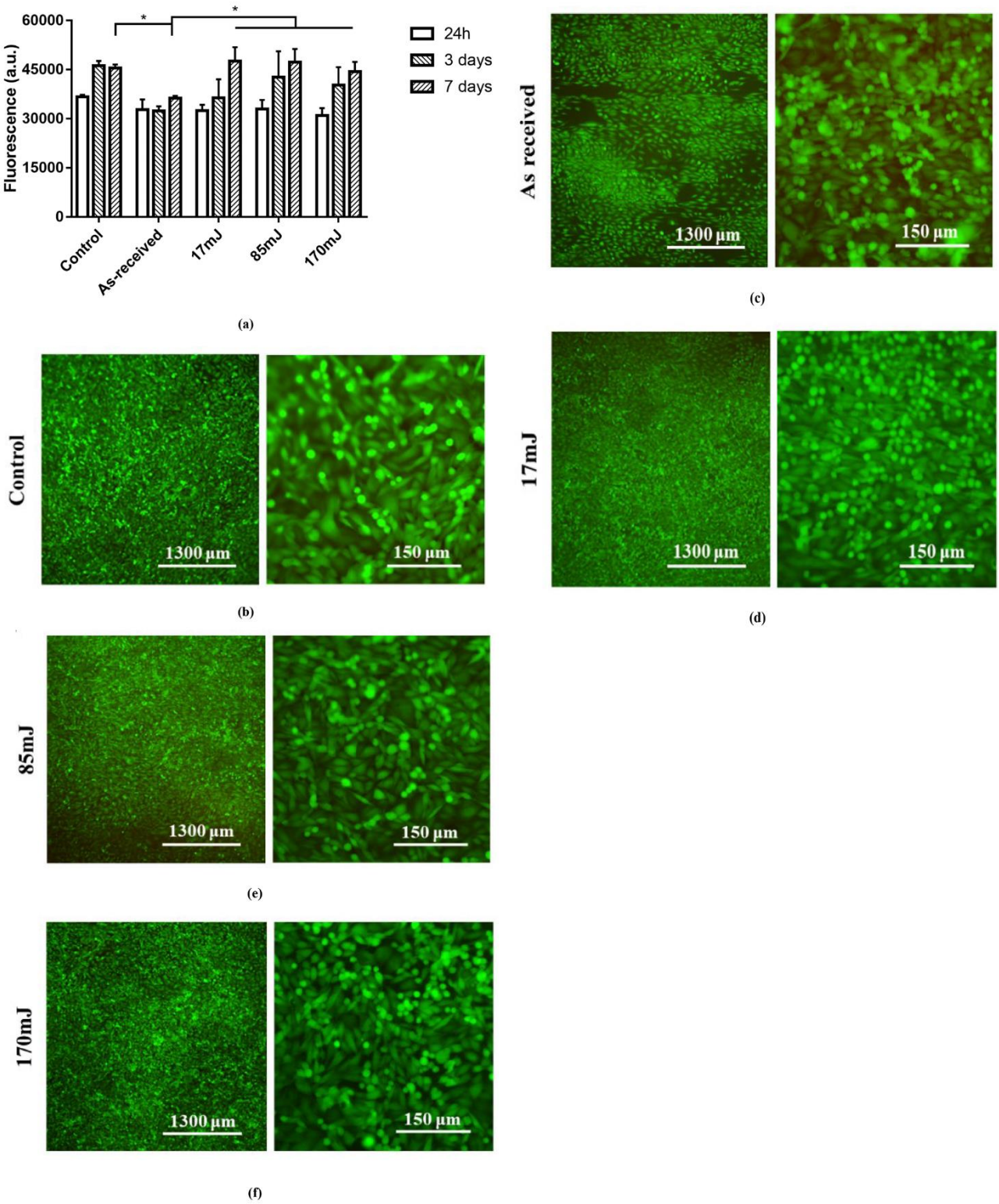

Figure 13 Biological response to human osteosarcoma cells (SAOS-2), including a) metabolic activity and Life/dead fluorescence images of cells after seven days of contact with b) control plastic slides and ZrO_2 ceramics in the c) as-received or laser peened, d) 17 mJ, e) 85 mJ and f) 170 mJ conditions where * signifies p-value <0.05 for alamar blue measurements after 7 days of seeding. Fluorescence images result from the merging of both GFP and Texas red channels.

This seems to be linked to the laser power as maximums of 47563 ± 3529 a.u. (where a.u. corresponds to arbitrary units in terms of fluorescence intensity) 47255 ± 3309 can be seen for the 17 mJ and 85 mJ samples with a slight reduction to 44428 ± 2426 a.u. as the laser power reached 170 mJ. Nevertheless, only statistical differences where observed between the as-received and all other groups, indicating that all laser shock treatment conditions significantly enhanced SAOS-2 metabolic activity. Moreover, SAOS-2 cells have been shown to continuously proliferate attaining full confluence and maturity after 7 or 14 days of seeding [44]. Given the large affinity for cell proliferation of the samples and the growth kinetics of SAOS-2 it seems likely that no influence on apoptosis may have resulted from the analysed surfaces.

Metabolic activity provides information about cell biochemical processes which can be correlated with cell viability, however, caution should be taken when linking metabolic activity with cell proliferation, growth and death [45]. To fully explore cell behaviour, live/dead staining was used on cells in all aforementioned samples after 7 days of contact (Figures 13 (b) to 13 (f)). Non-toxic controls (Figure 13 (b)) revealed homogeneously distributed cells divided in a lower confluent layer with branched and spread cells developing a top layer characterized by more circular cells. A similar bilayer can be observed in all the laser treated samples (Figures 13 (b) to 13 (f)), but the new top layer seems to be more developed on the 17 mJ and 85 mJ lower power substrates. This could explain the lower metabolic activity previously discussed. Similarly, the as-received ZrO_2 surface does not show a completely confluent initial monolayer, with some spaces of the base material visible and limited growing cells on top of the early monolayer. In all cases studied, no cells could be found red stained, suggesting that no loss in permeability and, consequently, damage was induced after 7 days. This coupled with the rise in metabolic activity indicates that all surfaces analysed are non-cytotoxic, suggesting that laser peening does not have any detrimental effect on the initial stages of cell proliferation.

4. Conclusions

This manuscript focused, on the effects of laser shock treatment/peening of ZrO_2 ceramics that has not previously been observed or reported in literature. Laser intensity was modified to map a processing window of laser shock treatment (LST). Through an increase in laser energy from 17 mJ to 170 mJ, we have found the damage threshold for ZrO_2 ceramics, correlating processing parameters with material microstructure and mechanical properties. More specifically, hardness, crack length and fracture toughness were analysed alongside the effect of LST treatment on the biological response of SAOS-2. The main findings of this work are summarized as:

- Metabolic activity measurements illustrated a rise in activity for all samples with increasing contact time from 24 h, 3 days and 7 days. The as-received surface reveals a more limited change in metabolism, but significant increase in cell activity in all laser peened samples relative to the as-received condition, suggested that this surface treatment enhanced cell response. As the laser energies increased, so did the cell response with 47563 ± 3529 a.u., 47255 ± 3309 observed for the 17 mJ and 85 mJ samples with a slight reduction to 44428 ± 2426 a.u., for the surface laser shock treated with 170 mJ. Results were more prominent with the same set of samples for metabolic activities. In all cases, no cells could be found “red stained”, which suggested that no loss in permeability and, consequent, damage was induced after 7-days. This was supported by a rise in metabolic activity indicated that all laser shock

treated surfaces were non-cytotoxic, meaning that laser shock treatment such as peening did not have any detrimental effect on the initial stages of cell proliferation.

- Optical microscopy revealed that surface of two of the three laser shock treated samples were cracked. The energy used was too high in those cases and it is proposed that the optimal laser energy to be used to obtain a crack free surface should be between 17 mJ and 85 mJ. The mechanically induced shock wave and corresponding detrimental effects over the surface with laser shock treatment at 170 mJ were far too intense, thus, lead to cracking. The effects under 17 mJ were not measurably, significant to undertake a detailed and timely investigation.
- The hardness was reduced in the three laser shock treated samples, with a reduction as high as 8%.
- Surface roughness was lowered for all laser shock treated surfaces with particularly lowest being with the highest laser energy applied and was attributed to material removal and flattening of the striations.
- Surface Fracture toughness (K_{IC}) was measured to be 4% higher for the 17 mJ, but was drastically decreased in the most damaged sample (170 mJ treated sample). These findings were not substantial over the top most surface, the material was not affected as much as it was within the deeper sub-surface as evidence from the incremental hole drilling measurements suggests.

Study of the residual stress induced in the material was also conducted by both incremental hole drilling method and hardness indentation method. The results from of the incremental hole drilling measurements showed the introduction of tensile residual stress at the surface in the three samples. . Furthermore, the depth at which the compressive residual stresses are located seem to also increase with the increase in laser energy. The observed measurement of tensile stress at the surface explained the measured reduction in degradation of the hardness, but the compressive residual stress induced deeper in the material indicate a level of micro-plastic deformation, in line with observations found in previous work on other ceramics.

Author Contributions

Dr. Pratik Shukla initiated the research and was instrumental in designing and conducting the laser shock treatment experiments, writing the paper, and undertaking all proposed changes post review. Mr. Vincent Zhang helped to conduct some of the laser shock treatment experiments and materials analysis – fracture toughness in particular. Dr. Xiaojun Shen conducted some of the laser shock treatment experiments and materials analysis – residual stress mesurement in particular. Dr. Victor M. Villapún conducted all the biological analysis of the LST samples. Dr. Sophie Cox facilitated the biological experimental investigation. Dr. Phil Swanson contributed to ensuring the technical accuracy within the paper and proof reading the manuscript to ensure grammatical accuracy.

Funding

The leading author of this paper would like to thank the Engineering Physical Sciences Research Council (EPSRC) funded laser loan pool scheme and also the Science & Technology Facilities Council (STFC) for granting a state-of-the-art system for Laser Shock Peening applications (Grant no: EP/G03088X/1, (13250017 - NSL4) Ultra-high energy 10J, Nd:YAG laser), which was made (by Litron

Lasers Ltd.) and deployed for the first-time by the leading author of this paper between the years 2014 to 2021.

Competing Interests

The authors declare that they have no conflict of interest.

References

1. Bajraktarova-Valjakova E, Korunoska-Stevkovska V, Kapusevska B, Gigovski N, Bajraktarova-Misevska C, Grozdanov A. Contemporary dental ceramic materials, a review: Chemical composition, physical and mechanical properties, indications for use. Open Access Maced J Medical Sci. 2018; 6: 1742-1755.
2. Birkby I, Stevens R. Applications of zirconia ceramics. Key Eng Mater. 1996; 122: 527-552.
3. Volpato CÂ, Garbelotto LG, Fredel MC, Bondioli F. Application of zirconia in dentistry: Biological, mechanical and optical considerations. In: Advances in ceramics-electric and magnetic ceramics, bioceramics, ceramics and environment. Rijeka: IntechOpen; 2011. pp. 397-420.
4. Yin L, Nakanishi Y, Alao AR, Song XF, Abduo J, Zhang Y. A review of engineered zirconia surfaces in biomedical applications. Procedia CIRP. 2017; 65: 284-290.
5. Scherrer SS, Mekki M, Crottaz C, Gahlert M, Romelli E, Marger L, et al. Translational research on clinically failed zirconia implants. Dent Mater. 2019; 35: 368-388.
6. Shukla PP, Lawrence J. Micro-shot peening of zirconia-advanced ceramic: An examination of surface integrity. J Mater Sci. 2015; 50: 1728-1739.
7. Schünemann FH, Galárraga-Vinueza ME, Magini R, Fredel M, Silva F, Souza JC, et al. Zirconia surface modifications for implant dentistry. Mater Sci Eng C. 2019; 98: 1294-1305.
8. Han J, Zhang F, Van Meerbeek B, Vleugels J, Braem A, Castagne S. Laser surface texturing of zirconia-based ceramics for dental applications: A review. Mater Sci Eng C. 2021; 123: 112034.
9. Shukla PP. Viability and characterization of the laser surface treatment of engineering ceramics. Loughborough: Loughborough University; 2011.
10. Shukla PP, Lawrence J, Wu H. Fracture toughness of a zirconia engineering ceramic and the effects thereon of surface processing with fibre laser radiation. Proc Inst Mech Eng B J Eng Manuf. 2010; 224: 1555-1569.
11. Shukla PP, Swanson PT, Page CJ. Laser shock peening and mechanical shot peening processes applicable for the surface treatment of technical grade ceramics: A review. Proc Inst Mech Eng B J Eng Manuf. 2014; 228: 639-652.
12. Gujba AK, Medraj M. Laser peening process and its impact on materials properties in comparison with shot peening and ultrasonic impact peening. Materials. 2014; 7: 7925-7974.
13. Clauer AH. Laser shock peening for fatigue resistance. In: Surface performance of titanium. Pittsburg: Minerals, Metals & Materials Society; 1996. pp. 217-230.
14. Hong X, Wang S, Guo D, Wu H, Wang J, Dai Y, et al. Confining medium and absorptive overlay: Their effects on a laser-induced shock wave. Opt Lasers Eng. 1998; 29: 447-455.
15. Ruschau JJ, John R, Thompson SR, Nicholas T. Fatigue crack nucleation and growth rate behavior of laser shock peened titanium. Int J Fatigue. 1999; 21: S199-S209.
16. Montross CS, Wei T, Ye L, Clark G, Mai YW. Laser shock processing and its effects on microstructure and properties of metal alloys: A review. Int J Fatigue. 2002; 24: 1021-1036.

17. Rubio-González C, Ocaña JL, Gomez-Rosas G, Molpeceres C, Paredes M, Banderas A, et al. Effect of laser shock processing on fatigue crack growth and fracture toughness of 6061-T6 aluminum alloy. Mater Sci Eng A. 2004; 386: 291-295.
18. Srinivasan S, Garcia DB, Gean MC, Murthy H, Farris TN. Fretting fatigue of laser shock peened Ti–6Al–4V. Tribol Int. 2009; 42: 1324-1329.
19. Zhang XC, Zhang YK, Lu JZ, Xuan FZ, Wang ZD, Tu ST. Improvement of fatigue life of Ti–6Al–4V alloy by laser shock peening. Mater Sci Eng A. 2010; 527: 3411-3415.
20. Zhang Y, You J, Lu J, Cui C, Jiang Y, Ren X. Effects of laser shock processing on stress corrosion cracking susceptibility of AZ31B magnesium alloy. Surf Coat Technol. 2010; 204: 3947-3953.
21. Schnick T, Steinhäuser S, Wielage B, Hofmann U, Tondu S, Peyre P, et al. Laser shock processing of Al-SiC composite coatings. J Therm Spray Technol. 1999; 8: 296-300.
22. Akita K, Sano Y, Takahashi K, Tanaka H, Ohya SI. Strengthening of Si_3N_4 ceramics by laser peening. Mater Sci Forum. 2006; 524: 141-146.
23. Zhang LF, Zhang YK, Feng AX. The fracture microphology of the ceramics by strong laser shock processing. Mater Sci Forum. 2006; 532: 137-140.
24. Longy F, Cagnoux J. Plasticity and microcracking in shock-loaded alumina. J Am Ceram Soc. 1989; 72: 971-979.
25. Acharya S, Bysakh S, Parameswaran V, Mukhopadhyay AK. Deformation and failure of alumina under high strain rate compressive loading. Ceram Int. 2015; 41: 6793-6801.
26. Bhattacharya M, Dalui S, Dey N, Bysakh S, Ghosh J, Mukhopadhyay AK. Low strain rate compressive failure mechanism of coarse grain alumina. Ceram Int. 2016; 42: 9875-9886.
27. Shukla P, Smith GC, Waugh DG, Lawrence L. Development in laser peening of advanced ceramics. In: Proc SPIE 9657, Industrial Laser Applications Symposium (ILAS 2015). Bellingham: SPIE; 2015. pp. 77-85.
28. Wang F, Zhang C, Lu Y, Nastasi M, Cui B. Laser shock processing of polycrystalline alumina ceramics. J Am Ceram Soc. 2017; 100: 911-919.
29. Shukla P, Nath S, Wang G, Shen X, Lawrence J. Surface property modifications of silicon carbide ceramic following laser shock peening. J Eur Ceram Soc. 2017; 37: 3027-3038.
30. Wang F, Zhang C, Yan X, Deng L, Lu Y, Nastasi M, et al. Microstructure-property relation in alumina ceramics during post-annealing process after laser shock processing. J Am Ceram Soc. 2018; 101: 4933-4941.
31. Wang F, Yan X, Zhang C, Deng L, Lu Y, Nastasi M, et al. Localized plasticity in silicon carbide ceramics induced by laser shock processing. Materialia. 2019; 6: 100265.
32. Shukla P, Robertson S, Wu H, Telang A, Kattoura M, Nath S, et al. Surface engineering alumina armour ceramics with laser shock peening. Mater Des. 2017; 134: 523-538.
33. Shukla P, Shen X, Allott R, Ertel K, Robertson S, Crookes R, et al. Response of silicon nitride ceramics subject to laser shock treatment. Ceram Int. 2021; 47: 34538-34553.
34. Shukla P, Crookes R, Wu H. Shock-wave induced compressive stress on alumina ceramics by laser peening. Mater Des. 2019; 167: 107626.
35. Al-Sanabani FA, Madfa AA, Al-Qudaimi NH. Alumina ceramic for dental applications: A review article. Am J Mater Res. 2014; 1: 26-34.
36. Gaviria L, Salcido JP, Guda T, Ong JL. Current trends in dental implants. J Korean Assoc Oral Maxillofac Surg. 2014; 40: 50-60.

37. Dawood RM, Ibraheem AF. Evaluation of shear bond strength of zirconia to tooth structure after different zirconia surface treatment techniques. J Baghdad Coll Dent. 2015; 325: 71234.
38. Manawi M, Ozcan M, Madina M, Cura C, Valandro LF. Impact of surface finishes on the flexural strength and fracture toughness of In-Ceram Zirconia. Gen Dent. 2012; 60: 138-142.
39. Ponton CB, Rawlings RD. Vickers indentation fracture toughness test Part 1 Review of literature and formulation of standardised indentation toughness equations. Mater Sci Technol. 1989; 5: 865-872.
40. Anstis GR, Chantikul P, Lawn BR, Marshall DB. A critical evaluation of indentation techniques for measuring fracture toughness: I, direct crack measurements. J Am Ceram Soc. 1981; 64: 533-538.
41. Shukla PP, Lawrence J. Fracture toughness modification by using a fibre laser surface treatment of a silicon nitride engineering ceramic. J Mater Sci. 2010; 45: 6540-6555.
42. Quinn G. Fracture toughness of ceramics by the Vickers indentation crack length method: A critical review. In: Mechanical properties and performance of engineering ceramics II: Ceramic engineering and science proceedings, Volume 27. Hoboken: John Wiley & Sons; 2006.
43. Breumier S, Villani A, Maurice C, Lévesque M, Kermouche G. Effect of crystal orientation on indentation-induced residual stress field: Simulation and experimental validation. Mater Des. 2019; 169: 107659.
44. Devendran C, Carthew J, Frith JE, Neild A. Cell adhesion, morphology, and metabolism variation via acoustic exposure within microfluidic cell handling systems. Adv Sci. 2019; 6: 1902326.
45. Pautke C, Schieker M, Tischer T, Kolk A, Neth P, Mutschler W, et al. Characterization of osteosarcoma cell lines MG-63, Saos-2 and U-2 OS in comparison to human osteoblasts. Anticancer Res. 2004; 24: 3743-3748.